

DESIGN AND PROTOTYPE TEST OF C-BAND STANDING-WAVE ACCELERATING STRUCTURE TO ENHANCE RF PHASE FOCUSING*

H. Yang[#], S. Shin, M. H. Cho, and W. Namkung
Pohang University of Science and Technology, Pohang 790-784, Korea

S. H. Kim
Argonne National Laboratory, Argonne, Illinois 60439, USA

J. S. Oh
National Fusion Research Institute, Daejeon 305-333, Korea

Abstract

A C-band standing-wave accelerator for X-ray and electron beam sources of medical radiotherapy is designed and being fabricated. The accelerator system is to be operated in two modes, using the X-ray and electron beams. Because of the energy loss in electron mode, the accelerator is capable of producing 6-MeV, 100-mA electron beams with peak 2-MW RF power, and 7.5-MeV, 20 mA electron beams with peak 2.5-MW RF power. The beam radius at the end of column was < 0.5 mm without focusing magnets in PARMELA simulations, because the bunching cells are designed to enhance the RF phase focusing. Each cavity in the bunching and normal cells was designed by the MWS code to maximize the effective shunt impedance with 3.8% inter-cell coupling in normal cells. The dimensions of normal cells were determined by the low power RF test of prototype cells with 5711.06-MHz resonant frequency and 3.5% inter-cell coupling. In this paper, we present details of the accelerator design and prototype test.

INTRODUCTION

In an electron linac for X-ray imaging and medical applications, the electron beam with 3 ~ 15 MeV, pulsed tens mA is required [1]. Also, these applications require the beam diameter of 1 – 2 mm at an X-ray conversion target for reducing the penumbra [2]. In order to achieve such a small beam diameter and a compact accelerator system, it requires an accelerating structure to maximize the RF focusing effect instead of adopting external focusing magnets.

A C-band electron accelerator system for the medical radiotherapy is being developed. It is able to produce both X-ray and electron beams. The X-ray beam is used to irradiate the viscera, and the electron beam is used to irradiate the inner and outer layers of skin. There is energy loss by scattering foils which are between the accelerator and the affected area in the electron mode (Fig. 1) [3]. Therefore, the accelerator is designed to produce 6-MeV, pulsed 100-mA electron beam with peak 2-MW power for X-ray beams, and 7.5-MeV, pulsed 50-mA electron beam with peak 2.5-MW power for electron beams. The bunching cells were designed with beam

dynamics simulation for enhancing the RF phase focusing [4]. We designed the RF cavities in the bi-periodic and on-axis-coupled accelerating structure with the MWS code. The dimensions of RF cavities in normal section were determined by the low power RF test with prototype aluminium cells.

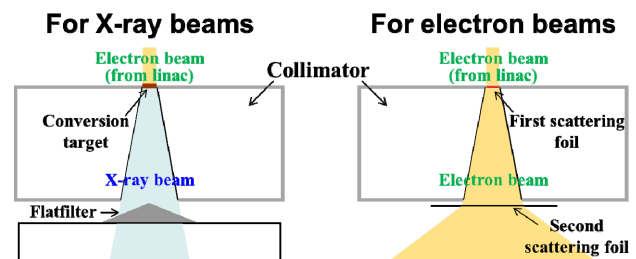


Figure 1: Schematic diagram of producing X-ray and electron beams.

Table 1: The Design Parameters of the Accelerator

| Parameters | X-ray beam | Electron beam |
|-------------------------------|------------------------------|---------------|
| Operating Frequency | 5712 MHz | |
| Input Pulsed RF Power | 2.0 MW | 2.5 MW |
| Pulse Length | 4 μ s | |
| Repetition Rate | 250 Hz | |
| E-gun Voltage | 19.0 kV | 20 kV |
| Input Pulsed Beam Current | 180 mA | 80 mA |
| Output Beam Energy | 6 MeV | 7.5 MeV |
| Output Pulsed Beam Current | 100 mA | 50 mA |
| Type of Structure | Bi-periodic, On-axis coupled | |
| Operating Mode | SW $\pi/2$ mode | |
| Beam Aperture Diameter* | 6 mm | |
| Average Accelerating Gradient | 134 MV/m | 167 MV/m |
| Number of Cells | 18 | |
| Inter-cell Coupling | 3.5% | |
| Quality Factor* | 9000 | |
| Shunt Impedance* | 113 M Ω /m | |
| Transit-time Factor* | 0.84 | |

*Values for normal cells.

*Work supported by the MOTIV, KIAT and LIDER, Korea.

[#]highlong@postech.ac.kr

ACCELERATOR SYSTEM

The accelerator system uses a 5712-MHz magnetron as an RF source. It is capable of producing a max. 2.5 MW RF with a 4- μ s pulse length and a 250-Hz repetition rate. It supplies pulsed 2.0 MW RF for X-ray beams, and pulsed 2.5 MW RF for electron beams (Table 1). The RF power is transmitted to the accelerating structure through the WR187 waveguide networks (Fig. 2). The pulsed modulator supplies a max. 50-kV and a 120-A pulsed power to the magnetron with a 4- μ s pulse length. It also supplies a max. 20-kV pulsed voltage to the E-gun.

The E-gun emits 80-mA electron beam with 20-kV pulse for electron beams, and 180-mA electron beam with 19-kV pulse for X-ray beams. The beam radius is 0.6 mm at the beam waist which is 15.2 mm from the anode. The direction of beams is adjusted by the steering coils in the upstream and downstream of the accelerating column (Fig. 2).

The accelerating column is attached to the E-gun directly (Fig. 3). For a compact structure, it has a built-in bunching section, and there is no pre-buncher and focusing magnet. A bi-periodic and an on-axis coupled structure is adopted for the $\pi/2$ -mode standing-wave structure [5]. The first three cells (Fig. 3) are the bunching cells with phase velocities (β_{ph}) of 0.3, 0.5, and 0.9. The number of normal cells with $\beta_{ph} = 1$ is 14 units, and after these, the coupler cell is attached to the tapered C-band waveguide.

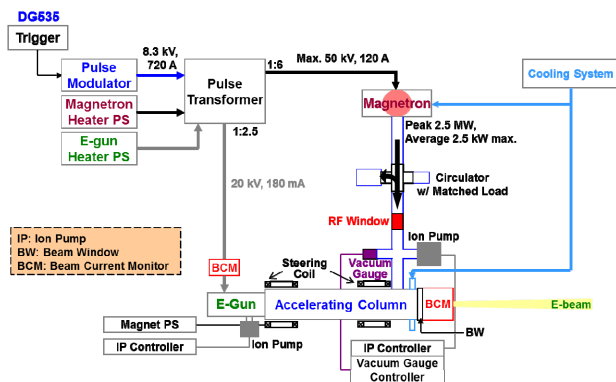


Figure 2: Schematic diagram of the accelerator system.

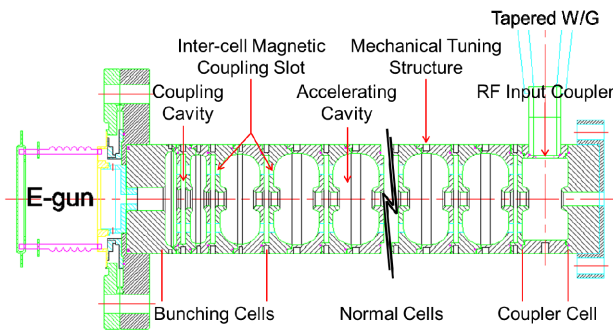


Figure 3: Cross-sectional view of the accelerating column.

BEAM DYNAMICS

Beam dynamics simulations were conducted by the PARMELA with input beams of 20-mm-mrad emittance. The phase velocities of bunching cells and the asymmetric geometry of the first and second bunching cells were optimized to enhance the RF phase focusing, in order to reduce the beam radius [6]. This optimization was conducted in the X-ray mode, because the beam size should be small in the X-ray mode for reducing the penumbra and beams are scattered at two foils in the electron mode [2].

Figure 4 is phase trajectories and beam envelopes in two modes. As a result of the optimization, the bunch is accelerated in the focusing region after the fifth cell (Fig. 4a), and the beam radius is less than 0.5 mm at the end of column in the X-ray mode (Fig. 4b). In the electron mode, the RF phase focusing is decreased, because the bunch is on crest through the normal cells (Fig 4a) [4]. However, the RF focusing is increased by increasing RF power and the space charge effect is reduced by less current than that in the X-ray mode. Therefore, the beam radius in the electron mode is almost the same as that in the X-ray mode. The output beam parameters of two modes are in Table 2. Since there is much beam loss in the flatfilter (Fig. 1), the beam current in the X-ray mode is higher than that in the electron mode, in order to obtain more radiation.

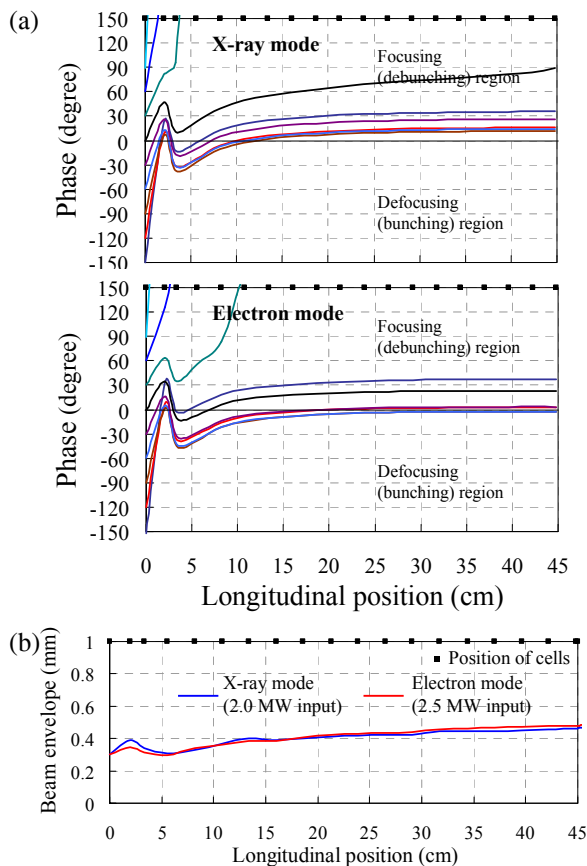


Figure 4: (a) The phase trajectories and (b) the beam envelopes of X-ray and electron modes.

Table 2: The Output Beam Parameters in X-ray and Electron Modes#

| Beam parameters | X-ray Mode | Electron mode |
|---------------------|------------|---------------|
| Average Energy | 6 MeV | 7.5 MeV |
| Pulsed Beam Current | 100 mA | 50 mA |
| Energy spread | 37% | 27% |
| Beam radius | ~ 0.5 mm | ~ 0.5 mm |

PROTOTYPE TEST

Each cell in the accelerating structure consists of the accelerating and coupling cavities. Magnetic coupling slots are bored on the side wall between the accelerating and coupling cavities for the inter-cell coupling. The inter-cell coupling constant was designed as 3.8%, restricted by the decrease of the shunt impedance. Due to these slots, the 3-D electromagnetic simulation was conducted with the MWS code to obtain the resonant frequency of each cavity (Fig. 5). To avoid field attenuations due to the stop band, the accelerating and coupling cavities should be designed for its frequency to be equal to the RF frequency [7].

To determine the cell dimension, the prototype tests were conducted with aluminium sample cells (Fig. 6). The resonant frequencies in Table 3 were measured with three sample cells. The first sample cell is fabricated by the result of the MWS simulation. By the comparison of the simulation and measurement, the final cell dimension is obtained (Table 3). In the final test, the resonant frequency of the $\pi/2$ -mode is 5711.06 MHz, the inter-cell coupling constant is 3.5%, and the frequency difference between the accelerating and coupling cavities is about 1 MHz which is calculated for the frequencies in 0 and π -modes [8].

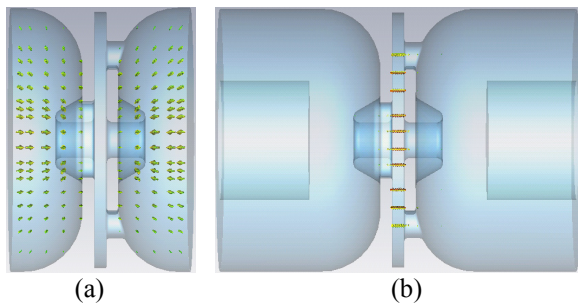


Figure 5: Simulation model to find the resonant frequency for (a): the accelerating cavity, (b): the coupling cavity.

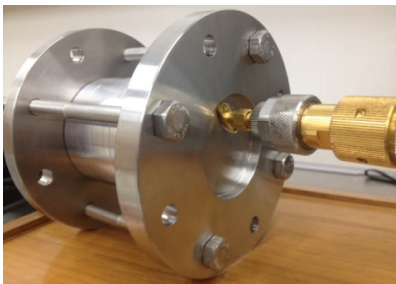


Figure 6: Prototype test with three Al sample cells.

Table 3: Resonant Frequencies of Sample Cells

| | RF frequency (MHz) | | |
|------------|--------------------|--------------|------------|
| | 0 mode | $\pi/2$ mode | π mode |
| Simulation | 5822.68 | 5711.00 | 5605.49 |
| Sample #1 | 5802.0 | 5704.5 | 5595.0 |
| Sample #2 | 5821.3 | 5705.3 | 5620.1 |
| Sample #3 | 5825.6 | 5720.7 | 5623.6 |
| Sample #4 | 5825.8 | 5711.8 | 5605.0 |
| Final | 5814.22 | 5711.06 | 5614.15 |

SUMMARY

We are developing a C-band standing-wave accelerator for X-ray and electron beam sources. It is capable of producing 6-MeV, 100-mA pulsed electron beams for X-ray beams, and 7.5-MeV, 50-mA pulsed electron beams for electron beams. The phase velocities of bunching cells and the geometry of the first and second bunching cell were optimized with beam dynamics simulations, in order to enhance the RF phase focusing. As a result, beam radius is less than 1 mm at the end of the column. The bi-periodic accelerating structure with on-axis coupling was designed with the MWS simulation. The dimensions of normal cells were determined with 5711.06 in $\pi/2$ -mode frequency and 3.5% inter-cell coupling by low power RF tests with prototype aluminium cells.

ACKNOWLEDGEMENT

This research is financially supported by the Ministry of Trade, Industry & Energy (MOTIV), Korea Institute for Advancement of Technology (KIAT) and Dongnam Institute for Regional Program Evaluation through the Leading Industry Development for Economic Region.

REFERENCES

- [1] C. Tang, et al., "Present Status of the Accelerator Industry in Asia," in *Proc. of IPAC10* (Kyoto, Japan, May 23-28, 2010), p. 2447.
- [2] L. W. Wang and K. Leszczynski, *Med. Phys.* **34**, No. 2, 485 (2007).
- [3] G. X. Ding, et al., *Med. Phys.* **23**, No. 3, 361 (1996).
- [4] H. Yang, et al., *Nucl. Inst. Meth. A* **703**, 145 (2013).
- [5] H. Euteneuer, et al., "The 4.9 GHz Accelerating Structure for MAMI C," in *Proc. of EPAC 2000* (Vienna, Austria, June 26-30, 2006), p. 1954.
- [6] H. Yang, et al., "Design of Compact C-band Standing-wave Accelerating structure Enhancing RF Phase Focusing," in *Proc. of IPAC12* (New Orleans, USA, May 20-25, 2012), p. 1221.
- [7] T. Shindake, "Analysis of the Transient Response in Periodic Structures Based on a Coupled-Resonator Model," in *Proc. of Joint US-CERN-Japan International School* (Tsukuba, Japan, Sep. 9-18, 1996), p. 1.
- [8] T. P. Wangler, *Principles of RF Linear Accelerators* (John Wiley & Sons, Inc., 1998).